



# Exploring the dynamics of lymphatic filariasis through a mathematical model and analysis with Holling type II treatment functions

F.A. Oguntolu, O.J. Peter\*, B.I. Omede, T.A. Ayoola and G.B. Balogun

\*Corresponding author

Received 22 July 2024; revised 16 November 2024; accepted 17 January 2025

Festus Abiodun Oguntolu<sup>1</sup>, festus.tolu@futminna.edu.ng

Olumuyiwa James Peter<sup>2</sup>, peterjames4real@gmail.com

Benjamin Idoko Omede<sup>3</sup>, benjaminomede197@gmail.com

Tawakalt Abosede Ayoola<sup>4</sup>, tawakalt.alade@uniosun.edu.ng

Ghaniyyat Bolanle Balogun<sup>5</sup>, balogun.gb@unilorin.edu.ng

<sup>1</sup>Department of Mathematics, Federal University of Technology, Minna, Niger State, Nigeria.

<sup>2</sup>Department of Mathematical and Computer Sciences, University of Medical Sciences, Ondo State, Nigeria.

Department of Epidemiology and Biostatistics, School of Public Health, University of Medical Sciences, Ondo State, Nigeria.

<sup>3</sup>Department of Mathematical Sciences, Prince Abubakar Audu (Formerly Kogi State) University, Anyigba, Nigeria.

<sup>4</sup>Department of Mathematical Sciences, Osun State University Osogbo, Nigeria.

<sup>5</sup>Department of Computer Science, University of Ilorin, Nigeria.

## How to cite this article

Oguntolu, F.A. Peter, O.J., Omede, B.I., Ayoola, T.A. and Balogun, G.B., Exploring the dynamics of lymphatic filariasis through a mathematical model and analysis with Holling type II treatment functions. *Iran. J. Numer. Anal. Optim.*, 2025; 15(2): 531-569. <https://doi.org/10.22067/ijnao.2025.89033.1482>

### Abstract

This paper presents a robust deterministic mathematical model incorporating Holling type II treatment functions to comprehensively investigate the dynamics of Lymphatic filariasis. Through qualitative analysis, the model demonstrates the occurrence of backward bifurcation when the basic reproduction number is less than one. Moreover, numerical simulations are employed to illustrate and validate key analytical findings. These simulation results emphasize the significance of accessible medical resources and the efficacy of prophylactic drugs in eradicating Lymphatic filariasis. The findings show that, enhancing medical resource availability and implementing effective treatment strategies in rural areas and regions vulnerable to Lymphatic filariasis is crucial for combating the transmission and control of this disease.

**AMS subject classifications (2020):** 92B05; 92D30; 92-10; 34D20

**Keywords:** Lymphatic filariasis; Holling type II treatment function; Reproduction number; Stability; Bifurcation.

## 1 Introduction

Lymphatic filariasis (LF), also known as Elephantiasis, is a neglected tropical disease that is prevalent in developing countries and disadvantaged communities across Sub-Sahara Africa, Asia, South and Central America, and the Pacific Island nations [22]. It is a parasitic disease transmitted through vectors and caused by three types of nematode parasites that reside in the lymphatic system: *Wuchereria bancrofti*, *Brugia Malayi*, and *B. timori*. *Wuchereria bancrofti* is responsible for the majority of cases worldwide, while *Brugia Malayi* and *B. timori* play significant roles as local causes in Southeast Asia. The transmission of these nematode parasites occurs through various species of mosquito vectors, including *Anopheles*, *Aedes*, *Culex*, *Mansonia*, and *Ochlerotatus* [8, 5]. The adult parasites take up residence in the lymphatic system of the human host. Following mating, they produce first stage larvae known as microfilariae, which then migrate to the peripheral blood circulation. These microfilariae exhibit a diurnal periodicity, residing in the

deep veins during the day and migrating to the peripheral circulation at night. The peak concentration of microfilariae in the peripheral blood occurs during a 4-hour timeframe from 10 p.m. to 4 a.m. This adaptation aligns with the biting behavior of the mosquito vectors [15, 10].

The extrinsic life cycle commences when the mosquito ingests microfilariae along with human blood during a bite. The microfilariae traverse the gut wall of the mosquito and reach the thoracic muscles, where they undergo a transformation, becoming shorter and thicker. These microfilariae progress into the first stage larvae (L1). Within a span of 5 to 7 days, the L1 larvae grow and develop into the more active second stage (L2). By approximately 10 to 11 days, they mature into infective stage larvae (L3) [1]. After reaching full maturity, the majority of infective larvae (L3) relocate to the proboscis of the mosquito, poised to infect another human [1]. This intricate life cycle involving mosquitoes as intermediaries is the primary means of transmitting LF. When a mosquito bites a human host, the L3 larvae are deposited on the skin's surface. Upon retracting its proboscis, the larvae enter the wound and travel to the lymphatic system. Approximately 9 to 10 days after entry, the L3 larvae molt and transform into fourth stage larvae (L4). The L4 stage undergoes further development, taking several days to a few months before reaching adulthood [1, 7, 12, 2].

In April 2012, LF was endemic in 73 countries and territories, putting an estimated 1.39 billion people at risk of infection, with approximately 120 million already infected [34]. Most infected individuals remain asymptomatic and are unaware of their condition unless tested [35]. However, these asymptomatic infections gradually cause damage to the lymphatic system, kidneys, and disrupt the body's immune system. The severity of symptoms is directly influenced by the patient's immune response and may manifest as acute inflammation of the lymphatic vessels, accompanied by high temperatures, chills, body aches, and swollen lymph nodes [1]. Excessive fluid accumulation in the affected tissues can occur [35, 13]. In chronic cases, LF leads to conditions such as lymphedema (tissue swelling) or elephantiasis (thickening of the skin), as well as swelling in the limbs and hydrocele (scrotal and breast swelling). In some instances, filarial abscesses may develop [1, 7, 12, 2].

In 2000, the World Health Organization (WHO) initiated the Global Program to Eliminate Lymphatic Filariasis (GPELF) with the ambitious target of eradicating LF by 2030. The strategy employed by the GPELF focuses on interrupting transmission through mass drug administration (MDA), while also addressing the suffering and disability caused by chronic manifestations of the disease [20, 36, 19]. The approach to interrupting transmission involves administering a combination of two drugs annually to the entire at-risk population. In areas without onchocerciasis, the treatment consists of albendazole (400mg) combined with diethylcarbamazine (6mg/kg) in areas where onchocerciasis and LF coexist [32, 27]. The mass administration of drugs typically extends over a period of 4-6 years, allowing sufficient time for adult parasites to exhaust their reproductive lifespan. However, in areas with low treatment coverage or high transmission intensity, longer campaigns may be necessary to ensure the interruption of transmission [27, 33].

Mathematical modeling has played a crucial role in understanding infectious diseases, although only a limited number of models have been developed specifically for studying the transmission dynamics and control of LF. For instance, Bhunu and Mushayabasa [3] created an epidemiological model to analyze the spread of LF. Their analysis of the reproduction number indicated that treatment would contribute to a reduction in LF cases, but the magnitude of the reduction was not quantified. Their numerical simulations suggested that effective LF control might require treatment for symptomatic individuals and chemoprophylaxis for those at risk. Mwamtobe et al. [21] formulated and analyzed a mathematical model for LF, incorporating intervention strategies. Their findings suggested that treatment led to a faster reduction in LF cases compared to quarantine. However, the greatest reduction occurred when both intervention approaches were implemented simultaneously. Oguntolu et al. [24] developed and rigorously analyzed a mathematical model for the transmission dynamics of LF, accounting for asymptomatic and symptomatic infections, as well as treatment. Their simulations demonstrated that a treatment coverage level of 75% among the human population was necessary to control LF. The successful elimination of LF by 2030 relies on the availability of medical resources and the implementation of effective treatments. In traditional epidemic models, the treatment rate for infected

individuals is often assumed to be constant or proportional to the number of infected cases. However, it is important to consider the limited availability of treatment resources within the community when determining an appropriate treatment rate for the disease [17]. Wang and Ruan [30] consider an SIR epidemic model with a constant treatment rate, the authors investigated the stability of the model and showed that the model exhibits various bifurcation. Furthermore, Zhou and Fan [37] modified the treatment rate to Holling type II, by varying the amount of medical resources and their supply efficiently, the target model admits both backward and Hopf bifurcation.

In this paper, our study focuses on the dynamics of how LF spreads and its control. This is the first research to examine the initial phase of infection by taking into account susceptible individuals who are undergoing prophylactic treatment. Furthermore, we have integrated a Holling type II treatment function at each stage of infection to enhance our understanding of the treatment and control strategies for LF. The rest of the paper is organized as follows: the model formulation and basic properties of the model described in section 2, the model analysis in section 3, the numerical analysis in section 4, and the concluding remarks in section 5.

## 2 Model formulations

The total human population at time  $t$ , denoted by  $N_H(t)$ , is sub-divided into seven mutually exclusive compartments of susceptible individuals not on prophylactic treatments  $S_H(t)$ , susceptible individuals on prophylactic treatments  $S_{HP}(t)$ , exposed individuals  $E_H(t)$ , L3-larvae stage (initial stage) infected individuals  $L(t)$ , acute stage infected individuals  $A(t)$ , Chronic stage infected individuals  $C(t)$  and treated individuals  $T(t)$ . So that

$$N_H(t) = S_H(t) + S_{HP}(t) + E_H(t) + L(t) + A(t) + C(t) + T(t).$$

The vector (mosquitoes) population at time  $t$ , denoted by  $N_V(t)$ , is sub-divided into three compartments of susceptible mosquitoes  $S_V(t)$ , exposed mosquitoes  $E_V(t)$ , and infectious mosquitoes  $I_V(t)$ . So that

$$N_V(t) = S_V(t) + E_V(t) + I_V(t).$$

The susceptible individuals not on prophylactic treatments  $S_H(t)$  is generated by birth or immigration at a constant rate  $\Pi_H$ . Susceptible individuals not on prophylactic treatments acquire LF infection through effective contact with infectious mosquitoes at the rate  $\lambda_H$ , given by

$$\lambda_H = \frac{\phi\beta_H I_V}{N_H},$$

where  $\phi$  is the mosquito-biting rate, and  $\beta_H$  is the transmission probability from  $I_V(t)$  to  $S_H(t)$ . The population of susceptible individuals on prophylactic treatments  $S_{HP}(t)$  is generated by susceptible individuals not on prophylactic treatments  $S_H(t)$  that started receiving prophylactic treatment at the rate  $\alpha$ , the susceptible individuals on prophylactic treatments acquire LF infection through effective contact with infectious mosquitoes at the rate  $(1 - \omega)\lambda_H$ , where  $\omega$  is the efficacy of the prophylaxis drugs. Exposed individuals progressed to the L3-larvae (initial stage of infection) stage at the rate  $\eta$ , L3-larvae stage infected individuals progressed to acute stage at the rate  $\sigma$ , and acute stage infected individuals progressed to chronic stage at the rate  $v$ . The human natural death rate  $\gamma_H$  is the same in all human compartments. We considered the Holling type II treatment functions  $f(L)$ ,  $f(A)$ , and  $f(C)$  for the L3-larvae stage infected individuals, the Acute stage infected individuals, and the Chronic stage infected individuals respectively, given by

$$f(L) = \frac{\tau_1 L}{1 + \varepsilon L}, \quad f(A) = \frac{\tau_2 A}{1 + \varepsilon A}, \quad \text{and} \quad f(C) = \frac{\tau_3 C}{1 + \varepsilon C},$$

where  $\tau_1$ ,  $\tau_2$ , and  $\tau_3$  are the treatment rates for L3-larvae stage, Acute stage, and Chronic stage infected individuals respectively, and  $\varepsilon$  is the limitation rate in medical resources availability. The population of the susceptible mosquitoes  $S_V(t)$ , is generated by the recruitment rate  $\Pi_V$ . Susceptible mosquitoes acquires LF infection through effective contact with infected individuals at the rate  $\lambda_V$ , given by

$$\lambda_V = \frac{\phi\beta_V (L + A + C)}{N_H},$$

where  $\beta_V$  is the transmission probability from infected individuals to susceptible mosquitoes and  $\phi$  is the mosquito-biting rate. The exposed mosquitoes

progressed to being infectious at the rate  $\rho$ . The death rate of mosquitoes is given by  $\gamma_V$ .

Based on the above formulation and assumptions, the LF model is given by the following system of deterministic nonlinear ordinary differential equations in (1) while the schematic diagram is presented in Figure 1. The description of the model state variables and parameters is presented in Table 1.

$$\begin{aligned}
 \frac{dS_H}{dt} &= \Pi_H - \frac{\phi\beta_H I_V S_H}{N_H} - (\alpha + \gamma_H) S_H + \kappa T, \\
 \frac{dS_{HP}}{dt} &= \alpha S_H - \frac{(1-\omega)\phi\beta_H I_V S_{HP}}{N_H} - \gamma_H S_{HP}, \\
 \frac{dE_H}{dt} &= \frac{\phi\beta_H I_V S_H}{N_H} + \frac{(1-\omega)\phi\beta_H I_V S_{HP}}{N_H} - (\eta + \gamma_H) E_H, \\
 \frac{dL}{dt} &= \eta E - \frac{\tau_1 L}{1 + \varepsilon L} - (\sigma + \gamma_H) L, \\
 \frac{dA}{dt} &= \sigma L - \frac{\tau_2 A}{1 + \varepsilon A} - (v + \gamma_H) A, \\
 \frac{dC}{dt} &= v A - \frac{\tau_3 C}{1 + \varepsilon C} - \gamma_H C, \\
 \frac{dT}{dt} &= \frac{\tau_1 L}{1 + \varepsilon L} + \frac{\tau_2 A}{1 + \varepsilon A} + \frac{\tau_3 C}{1 + \varepsilon C} - (\kappa + \gamma_H) T, \\
 \frac{dS_V}{dt} &= \Pi_V - \frac{\phi\beta_V (L + A + C) S_V}{N_H} - \gamma_V S_V, \\
 \frac{dE_V}{dt} &= \frac{\phi\beta_V (L + A + C) S_V}{N_H} - (\rho + \gamma_V) E_V, \\
 \frac{dI_V}{dt} &= \rho E_V - \gamma_V I_V.
 \end{aligned} \tag{1}$$

## 2.1 Basic properties of the model

### 2.1.1 Positivity and boundedness of solution

In order for the model (1) to be biological and mathematically meaningful, it is pertinent to show that the state variables of the model are nonnegative for all time  $t > 0$ .

**Theorem 1.** Let the initial data be  $S_H(0) \geq 0$ ,  $S_{HP}(0) \geq 0$ ,  $E_H(0) \geq 0$ ,  $L(0) \geq 0$ ,  $A(0) \geq 0$ ,  $C(0) \geq 0$ ,  $T(0) \geq 0$ ,  $S_V(0) \geq 0$ ,  $E_V(0) \geq 0$ , and

Table 1: Description of the model state variables and parameters

Variable	Description
$S_H$	Susceptible individuals not on prophylactic treatment.
$S_{HP}$	Susceptible individuals on prophylactic treatment.
$E_H$	Exposed individuals.
$L$	L3-larvae stage (initial stage) infected individuals.
$A$	Acute stage infected individuals.
$C$	Chronic stage infected individuals.
$T$	Treated individuals.
$S_V$	Susceptible mosquitoes.
$E_V$	Exposed mosquitoes.
$I_V$	Infectious mosquitoes.
Parameter	Description
$\Pi_H$	Recruitment rate for humans.
$\Pi_V$	Recruitment rate for mosquitoes.
$\phi$	Mosquito biting rate.
$\beta_H$	Transmission probability from $I_V$ to $S_H$ .
$\beta_V$	Transmission probability from $L$ , $A$ , and $C$ to $S_V$ .
$\gamma_H$	Natural death rate for humans.
$\gamma_V$	Death rate for mosquitoes.
$\alpha$	Progression rate from $S_H$ to $S_{HP}$ .
$\sigma$	Progression rate from $L$ to $A$ .
$\omega$	Efficacy of prophylaxis drugs.
$\eta$	Progression rate from $E_H$ to $L$ .
$\nu$	Progression rate from $A$ to $C$ .
$\tau_1$	Treatment rate of L3-larvae stage infection.
$\tau_2$	Treatment rate of Acute stage infection.
$\tau_3$	Treatment rate of Chronic stage infection.
$\varepsilon$	Limitation rate in medical resources availability.
$\kappa$	Rate at which treated individuals becomes susceptible again.
$\rho$	Progression rate from $E_V$ to $I_V$ .

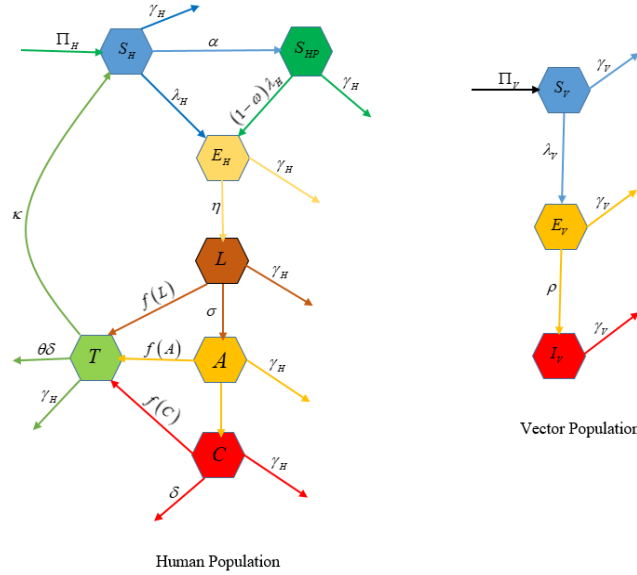


Figure 1: Schematic diagram of the flowchart

$I_V(0) \geq 0$ . Then, the solution  $(S_H, S_{HP}, E_H, L, A, C, T, S_V, E_V, I_V)$  to the model (1) is nonnegative for all  $t > 0$ .

*Proof.* Let  $t_1 = \sup\{t > 0 : S_H(t) > 0, S_{HP}(t) > 0, E_H(t) > 0, L(t) > 0, A(t) > 0, C(t) > 0, T(t) > 0, S_V(t) > 0, E_V(t) > 0, I_V(t) > 0 \in [0, t]\}$ . Then  $t_1 > 0$ . We have from the first equation of the model (1) that

$$\frac{dS_H}{dt} = \Pi_H - \lambda_H S_H - (\alpha + \gamma_H) S_H + \kappa T.$$

Solving the equation above, we have

$$\begin{aligned} & \frac{d}{dt} \left\{ S_H(t) \left[ \exp \left( \int_0^t \lambda_H(\zeta) d\zeta + (\alpha + \gamma_H) t \right) \right] \right\} \\ &= (\Pi_H + \kappa T) \times \exp \left( \int_0^t \lambda_H(\zeta) d\zeta + (\alpha + \gamma_H) t \right). \end{aligned}$$

Integrating the above equations at the range  $[0, t_1]$ , we obtained

$$\begin{aligned} & \left\{ S_H(t_1) \exp \left[ \int_0^{t_1} \lambda_H(\zeta) d\zeta + (\alpha + \gamma_H) t_1 \right] \right\} - S_H(0) \\ &= (\Pi_H + \kappa T) \times \int_0^{t_1} \exp \left[ \int_0^x \lambda_H(\zeta) d\zeta + (\alpha + \gamma_H) x \right] dx. \end{aligned}$$

So that

$$\begin{aligned}
 S_H(t_1) = & S_H(0) \exp \left[ - \left( \int_0^{t_1} \lambda_H(\zeta) d\zeta + (\alpha + \gamma_H) t_1 \right) \right] \\
 & + \exp \left[ - \left( \int_0^{t_1} \lambda_H(\zeta) d\zeta + (\alpha + \gamma_H) t_1 \right) \right] \\
 & \times (\Pi_H + \kappa T) \int_0^{t_1} \exp \left[ \int_0^x \lambda_H(\zeta) d\zeta + (\alpha + \gamma_H) x \right] dx > 0.
 \end{aligned}$$

Similarly, it can be shown that  $S_{HP} > 0, E_H > 0, L > 0, A > 0, C > 0, T > 0, S_V > 0, E_V > 0, I_V > 0$ . □

### 2.1.2 Invariant region

We considered that the region in which the solution of the LF model (1) is feasible, given by

$$\Omega = \Omega_H \times \Omega_V \subset \mathbb{R}_+^7 \times \mathbb{R}_+^3, \tag{2}$$

where

$$\Omega_H = \left\{ (S_H, S_{HP}, E_H, L, A, C, T) \in \mathbb{R}_+^7 : N_H \leq \frac{\Pi_H}{\gamma_H} \right\},$$

and

$$\Omega_V = \left\{ (S_V, E_V, I_V) \in \mathbb{R}_+^3 : N_V \leq \frac{\Pi_V}{\gamma_V} \right\}.$$

**Lemma 1.** The region  $\Omega = \{(S_H, S_{HP}, E_H, L, A, C, T, S_V, E_V, I_V) \in \mathbb{R}_+^{10} : N_H \leq \frac{\Pi_H}{\gamma_H}, N_V \leq \frac{\Pi_V}{\gamma_V}\}$  is positively invariant for the model (1).

*Proof.* By adding the human and vector compartments of the model system (1), we obtained

$$\begin{aligned}
 \frac{dN_H}{dt} &= \Pi_H - \gamma_H N_H, \\
 \frac{dN_V}{dt} &= \Pi_V - \gamma_V N_V.
 \end{aligned} \tag{3}$$

Thus, the standard comparison theorem [18] is used to show that

$$\begin{aligned}
 N_H(t) &\leq N_H(0) e^{-\gamma_H t} + \frac{\Pi_H}{\gamma_H} (1 - e^{-\gamma_H t}), \\
 N_V(t) &\leq N_V(0) e^{-\gamma_V t} + \frac{\Pi_V}{\gamma_V} (1 - e^{-\gamma_V t}).
 \end{aligned} \tag{4}$$

In particular, if  $N_H(0) \leq \frac{\Pi_H}{\gamma_H}$  and  $N_V(0) \leq \frac{\Pi_V}{\gamma_V}$ , then  $N_H(t) \leq \frac{\Pi_H}{\gamma_H}$  and  $N_V(t) \leq \frac{\Pi_V}{\gamma_V}$ . Therefore, the region  $\Omega$  is a positively-invariant (that is, the solutions to the model remain positive for all time  $t$ ) and the model is well posed and biologically meaningful.  $\square$

### 3 Model analysis

In this section, we shall be analyzing the model for the stability of the disease-free equilibrium (DFE) and endemic equilibrium.

#### 3.1 Disease-free equilibrium (DFE)

The DFE points are steady state solutions where there is no LF infection in the community. This is achieved by setting the infected compartments to zero (that is,  $E_H = L = A = C = T = E_V = I_V = 0$ ) and setting the right-hand side of the model system (1) to zero. Therefore, the DFE point,  $(\xi_0)$ , is given by

$$\xi_0 = (S_H^*, S_{HP}^*, E_H^*, L^*, A^*, C^*, T^*, S_V^*, E_V^*, I_V^*) = (S_H^*, S_{HP}^*, 0, 0, 0, 0, 0, S_V^*, 0, 0), \quad (5)$$

where

$$S_H^* = \frac{\Pi_H}{\alpha + \gamma_H}, S_{HP}^* = \frac{\alpha \Pi_H}{(\alpha + \gamma_H) \gamma_H}, \text{ and } S_V^* = \frac{\Pi_V}{\gamma_V}.$$

#### 3.2 Basic reproduction number

The basic reproductive number  $R_0$  is a measurement of the potential for the spreading disease in a population. Mathematically,  $R_0$  is a threshold parameter for the stability of a DFE and is related to the peak and final size of an epidemic. It is defined as the expected number of secondary cases of infection, which would occur due to a primary case in a completely susceptible population [9, 29]. It is an important parameter that governs the spread of a disease.

The reproductive number ( $R_0$ ) can be computed using the next generation operator method described in [9, 29]. Using the matrices  $F$  and  $V$ , for the new infection and the remaining transition terms, respectively,

$$F = \begin{bmatrix} 0 & 0 & 0 & 0 & 0 & 0 & \frac{\phi\beta_H(S_H^*+(1-\omega)S_{HP}^*)}{N_H} \\ 0 & 0 & 0 & 0 & 0 & 0 & 0 \\ 0 & 0 & 0 & 0 & 0 & 0 & 0 \\ 0 & 0 & 0 & 0 & 0 & 0 & 0 \\ 0 & 0 & 0 & 0 & 0 & 0 & 0 \\ 0 & \frac{\phi\beta_V S_V^*}{N_H} & \frac{\phi\beta_V S_V^*}{N_H} & \frac{\phi\beta_V S_V^*}{N_H} & 0 & 0 & 0 \\ 0 & 0 & 0 & 0 & 0 & 0 & 0 \end{bmatrix},$$

and

$$V = \begin{bmatrix} (\eta + \gamma_H) & 0 & 0 & 0 & 0 & 0 & 0 \\ -\eta & (\sigma + \tau_1 + \gamma_H) & 0 & 0 & 0 & 0 & 0 \\ 0 & -\sigma & (\nu + \tau_2 + \gamma_H) & 0 & 0 & 0 & 0 \\ 0 & 0 & -\nu & (\tau_3 + \gamma_H) & 0 & 0 & 0 \\ 0 & -\tau_1 & -\tau_2 & -\tau_3 & (\kappa + \gamma_H) & 0 & 0 \\ 0 & 0 & 0 & 0 & 0 & (\rho + \gamma_V) & 0 \\ 0 & 0 & 0 & 0 & 0 & -\rho & \gamma_V \end{bmatrix}.$$

Hence, it follows from [9] that  $R_0 = \rho(FV^{-1})$ , where  $\rho$  is the spectral radius or largest eigenvalues of  $(FV^{-1})$ .

Therefore,

$$R_0 = \sqrt{\frac{\Pi_V \gamma_H \phi^2 \beta_V \beta_H (\gamma_H + (1 - \omega) \alpha) (\sigma (v + B_5) + B_4 B_5) \eta \rho}{\Pi_H \gamma_V^2 B_1 B_2 B_3 B_4 B_5 B_7}}, \quad (6)$$

where

$$B_1 = \alpha + \gamma_H, \quad B_2 = \eta + \gamma_H, \quad B_3 = \sigma + \tau_1 + \gamma_H, \quad B_4 = v + \tau_2 + \gamma_H, \\ B_5 = \tau_3 + \gamma_H, \quad B_6 = \kappa + \gamma_H, \quad \text{and} \quad B_7 = \rho + \gamma_V.$$

### 3.3 Local stability of the DFE

**Theorem 2.** The DFE  $(\xi_0)$  of the model (1) is locally asymptotically stable if  $R_0 < 1$ , and unstable if  $R_0 > 1$ .

*Proof.* The local stability of the DFE  $(\xi_0)$  of the model (1) is analyzed by the Jacobian matrix of the model system (1) evaluated at the DFE  $(\xi_0)$ , given by

$$J(\xi_0) = \begin{bmatrix} -B_1 & 0 & 0 & 0 & 0 & 0 & \kappa & 0 & 0 & -\frac{\phi \beta_H \gamma_H}{B_1} \\ \alpha & -\gamma_H & 0 & 0 & 0 & 0 & 0 & 0 & 0 & -\frac{\phi \beta_H D_1}{B_1} \\ 0 & 0 & -B_2 & 0 & 0 & 0 & 0 & 0 & 0 & -\frac{\phi \beta_H D_2}{B_1} \\ 0 & 0 & \eta & -B_3 & 0 & 0 & 0 & 0 & 0 & 0 \\ 0 & 0 & 0 & \sigma & -B_4 & 0 & 0 & 0 & 0 & 0 \\ 0 & 0 & 0 & 0 & \nu & -B_5 & 0 & 0 & 0 & 0 \\ 0 & 0 & 0 & \tau_1 & \tau_2 & \tau_3 & -B_6 & 0 & 0 & 0 \\ 0 & 0 & 0 & -D_3 & -D_3 & -D_3 & 0 & -\gamma_V & 0 & 0 \\ 0 & 0 & 0 & D_3 & D_3 & D_3 & 0 & 0 & -B_7 & 0 \\ 0 & 0 & 0 & 0 & 0 & 0 & 0 & 0 & \rho & -\gamma_V \end{bmatrix},$$

where  $B_1 = \alpha + \gamma_H$ ,  $B_2 = \eta + \gamma_H$ ,  $B_3 = \sigma + \tau_1 + \gamma_H$ ,  $B_4 = v + \tau_2 + \gamma_H$ ,  $B_5 = \tau_3 + \gamma_H$ ,  $B_6 = \kappa + \gamma_H$ ,  $B_7 = \rho + \gamma_V$ ,  $D_1 = (1 - \omega)\alpha$ ,  $D_2 = \gamma_H + (1 - \omega)\alpha$ , and  $D_3 = \frac{\phi\beta_V\Pi_V\gamma_H}{\Pi_H\gamma_V}$ .

The eigenvalues of the Jacobian matrix  $J(\xi_0)$  are  $\lambda_1 = -\gamma_H$ ,  $\lambda_2 = -B_1$ ,  $\lambda_3 = -B_6$ ,  $\lambda_4 = -\gamma_V$  and the roots of the characteristic polynomial below:

$$P(\lambda) = \lambda^6 + a_1\lambda^5 + a_2\lambda^4 + a_3\lambda^3 + a_4\lambda^2 + a_5\lambda + a_6, \quad (7)$$

where

$$\begin{aligned} a_1 &= B_2 + B_3 + B_4 + B_5 + B_7 + \gamma_V, \\ a_2 &= B_2(B_3 + B_4 + B_5 + B_7 + \gamma_V) + B_3(B_4 + B_5 + B_7 + \gamma_V) + B_7\gamma_V \\ &\quad + B_4(B_5 + B_7 + \gamma_V) + B_5(B_7 + \gamma_V), \\ a_3 &= B_2B_3(B_4 + B_5 + B_7 + \gamma_V) + (B_2B_4 + B_3B_4)(B_5 + B_7 + \gamma_V) \\ &\quad + (B_7 + \gamma_V)(B_2B_5 + B_3B_5) + B_7\gamma_V(B_2 + B_3 + B_4 + B_5) \\ &\quad + B_4B_5(B_7 + \gamma_V), \\ a_4 &= \gamma_V(B_2B_3(B_4 + B_5 + B_7) + B_4(B_2 + B_3)(B_5 + B_7)) \\ &\quad + \gamma_V B_5 B_7 (B_2 + B_3 + B_4) + B_2 B_3 B_4 (B_5 + B_7) \\ &\quad + B_5 B_7 (B_2 (B_3 + B_4) + B_3 B_4) - \frac{\Pi_V \gamma_H \phi^2 \beta_H \beta_V D_2 \eta \rho}{\Pi_H \gamma_V B_1}, \\ a_5 &= \gamma_V (B_2 B_3 (B_4 B_5 + B_4 B_7 + B_5 B_7) + B_4 B_5 B_7 (B_2 + B_3)) \\ &\quad + B_2 B_3 B_4 B_5 B_7 - \frac{\Pi_V \gamma_H \phi^2 \beta_H \beta_V D_2 \eta \rho (\sigma + B_4 + B_5)}{\Pi_H \gamma_V B_1}, \\ a_6 &= \gamma_V B_2 B_3 B_4 B_5 B_7 (1 - R_0^2). \end{aligned}$$

Applying the Routh–Hurwitz criterion [23], which states that all roots of the polynomial (7) have negative real parts if and only if the coefficient of  $a_i > 0$ , for  $i = 1, 2, 3, 4, 5, 6$ . Clearly, for  $a_6 > 0$  then  $R_0 < 1$ . Therefore, all the eigenvalues of the Jacobian matrix  $J(\xi_0)$  have negative real parts when  $R_0 < 1$  and the DFE point is locally asymptotically stable.  $\square$

Biologically, the implication of Theorem 2 is that a small influx of LF infected individuals in the population will not cause an LF outbreak as long as the reproduction number ( $R_0$ ) is less than unity [26]. It is important to

note that this result depends on the initial sizes of the infected individuals in the population.

### 3.4 Existence of an endemic equilibrium

In this section, we shall investigate the existence of an endemic equilibrium point. The endemic equilibrium is a steady state where the disease persists in the population. In this case, the infected variables are nonzero (that is,  $E_H \neq 0, L \neq 0, A \neq 0, C \neq 0, T \neq 0, E_V \neq 0, I_V \neq 0$ ). We shall be investigating the endemic equilibrium using the “forces of infection”, given by

$$\lambda_H^{**} = \frac{\phi\beta_H I_V^{**}}{N_H^{**}}, \text{ and } \lambda_V^{**} = \frac{\phi\beta_V (L^{**} + A^{**} + C^{**})}{N_H^{**}}, \tag{8}$$

where

$$N_H^{**} = S_H^{**} + S_{HP}^{**} + E_H^{**} + L^{**} + A^{**} + C^{**} + T^{**}.$$

The equations of the model system (1) are equated to zero and solved to get an expression of each of the model variables in terms of the forces of infection. For convenience, we let  $\varepsilon L^{**} = Z_1, \varepsilon A^{**} = Z_2$ , and  $\varepsilon C^{**} = Z_3$ . So that

$$\begin{aligned} S_H^{**} &= \frac{\Pi_H B_2 B_6 ((1-\omega)\lambda_H^{**} + \gamma_H) Q_1}{B_2 B_6 (\lambda_H^{**} + B_1) ((1-\omega)\lambda_H^{**} + \gamma_H) Q_1 - \lambda_H^{**} \kappa \eta ((1-\omega)(\lambda_H^{**} + \alpha) + \gamma_H) Q_2}, \\ S_{HP}^{**} &= \frac{\alpha \Pi_H B_2 B_6 Q_1}{B_2 B_6 (\lambda_H^{**} + B_1) ((1-\omega)\lambda_H^{**} + \gamma_H) Q_1 - \lambda_H^{**} \kappa \eta ((1-\omega)(\lambda_H^{**} + \alpha) + \gamma_H) Q_2}, \end{aligned} \tag{9}$$

$$\begin{aligned} E_H^{**} &= \frac{\lambda_H^{**} \Pi_H B_6 ((1-\omega)(\lambda_H^{**} + \alpha) + \gamma_H) Q_1}{B_2 B_6 (\lambda_H^{**} + B_1) ((1-\omega)\lambda_H^{**} + \gamma_H) Q_1 - \lambda_H^{**} \kappa \eta ((1-\omega)(\lambda_H^{**} + \alpha) + \gamma_H) Q_2}, \\ L^{**} &= \frac{\lambda_H^{**} \Pi_H B_6 \eta (1 + Z_1) ((1-\omega)(\lambda_H^{**} + \alpha) + \gamma_H) Q_3}{B_2 B_6 (\lambda_H^{**} + B_1) ((1-\omega)\lambda_H^{**} + \gamma_H) Q_1 - \lambda_H^{**} \kappa \eta ((1-\omega)(\lambda_H^{**} + \alpha) + \gamma_H) Q_2}, \\ A^{**} &= \frac{\lambda_H^{**} \Pi_H B_6 \eta \sigma (1 + Z_1) (1 + Z_2) ((1-\omega)(\lambda_H^{**} + \alpha) + \gamma_H) (B_5 + \gamma_H Z_3)}{B_2 B_6 (\lambda_H^{**} + B_1) ((1-\omega)\lambda_H^{**} + \gamma_H) Q_1 - \lambda_H^{**} \kappa \eta ((1-\omega)(\lambda_H^{**} + \alpha) + \gamma_H) Q_2}, \\ C^{**} &= \frac{\lambda_H^{**} \Pi_H B_6 \eta \sigma v (1 + Z_1) (1 + Z_2) (1 + Z_3) ((1-\omega)(\lambda_H^{**} + \alpha) + \gamma_H)}{B_2 B_6 (\lambda_H^{**} + B_1) ((1-\omega)\lambda_H^{**} + \gamma_H) Q_1 - \lambda_H^{**} \kappa \eta ((1-\omega)(\lambda_H^{**} + \alpha) + \gamma_H) Q_2}, \\ T^{**} &= \frac{\lambda_H^{**} \Pi_H \eta ((1-\omega)(\lambda_H^{**} + \alpha) + \gamma_H) Q_2}{B_2 B_6 (\lambda_H^{**} + B_1) ((1-\omega)\lambda_H^{**} + \gamma_H) Q_1 - \lambda_H^{**} \kappa \eta ((1-\omega)(\lambda_H^{**} + \alpha) + \gamma_H) Q_2}, \\ S_V^{**} &= \frac{\Pi_V}{\lambda_V^{**} + \gamma_V}, E_V^{**} = \frac{\lambda_V^{**} \Pi_V}{(\lambda_V^{**} + \gamma_V) B_7}, \text{ and } I_V^{**} = \frac{\lambda_V^{**} \Pi_V \rho}{(\lambda_V^{**} + \gamma_V) B_7 \gamma_V}, \end{aligned} \tag{10}$$

where

$$B_1 = \alpha + \gamma_H, B_2 = \eta + \gamma_H, B_3 = \sigma + \tau_1 + \gamma_H, B_4 = v + \tau_2 + \gamma_H, \\ B_5 = \tau_3 + \gamma_H, B_6 = \kappa + \gamma_H, B_7 = \rho + \gamma_V,$$

$$Q_1 = (B_3 + (\sigma + \gamma_H) Z_1) (B_4 + (v + \gamma_H) Z_2) (B_5 + \gamma_H Z_3), \\ Q_2 = \tau_1 (B_4 + (v + \gamma_H) Z_2) (B_5 + \gamma_H Z_3) + \tau_2 \sigma (1 + Z_1) (B_5 + \gamma_H Z_3) + \\ \tau_3 \sigma v (1 + Z_1) (1 + Z_2), \text{ and } Q_3 = (B_4 + (v + \gamma_H) Z_2) (B_5 + \gamma_H Z_3).$$

Substituting (9) into (8), we obtained

$$f(\lambda_H^{**}) = P_1 \lambda_H^{**4} + P_2 \lambda_H^{**3} + P_3 \lambda_H^{**2} + P_4 \lambda_H^{**} + P_5, \tag{11}$$

where  $P_1 = \Pi_H^2 B_7 \gamma_V (1 - \omega)^2 (\phi \beta_V B_6 e_1 + \gamma_V e_2) e_2$ ,  $P_2 = K_1 + K_2 - K_3$ ,  $P_3 = K_4 + K_5 + K_6 - (K_7 + K_8)$ ,  $P_4 = K_9 + K_{10} - K_{11}$ , and  $P_5 = \Pi_H^2 \gamma_V^2 B_1^2 B_6^2 B_7 y_1^2 y_2^2 y_3^2 \left( 1 - \frac{\Pi_H \Pi_V \phi^2 \beta_H \beta_V B_1 B_2 B_6^2 \gamma_H \rho Q_1 e_1 (B_1 - \alpha \omega)}{\Pi_H^2 \gamma_V^2 B_1^2 B_6^2 B_7 y_1^2 y_2^2 y_3^2} \right)$ , with

$$K_1 = \Pi_H^2 B_7 \gamma_V e_2 (B_1 - \alpha \omega) (1 - \omega) (\phi \beta_V B_6 e_1 + \gamma_V e_2) \\ + \Pi_H^2 B_2 B_6 B_7 \gamma_V y_1 y_2 y_3 (1 - \omega)^2 (\phi \beta_V B_6 e_1 + \gamma_V e_2), \\ K_2 = \Pi_H^2 B_7 \gamma_V (\phi \beta_V B_6 e_1 (B_1 - \alpha \omega) + \gamma_V (1 - \omega) e_2) (1 - \omega) e_2, \\ K_3 = \Pi_H \Pi_V \phi^2 \beta_V \beta_H B_6 \rho e_1 e_3 (1 - \omega), \\ K_4 = \Pi_H^2 B_7 \gamma_V (1 - \omega) (\phi \beta_V B_6 e_1 + \gamma_V e_2) B_1 B_2 B_6 y_1 y_2 y_3, \\ K_5 = \Pi_H^2 B_2 B_6 B_7 \gamma_V y_1 y_2 y_3 (1 - \omega) (\phi \beta_V B_6 e_1 (B_1 - \alpha \omega) + \gamma_V e_2 (1 - \omega)) \\ + \Pi_H^2 B_7 \gamma_V e_2 (B_1 - \alpha \omega) (\phi \beta_V B_6 e_1 (B_1 - \alpha \omega) + \gamma_V e_2 (1 - \omega)), \\ K_6 = \Pi_H^2 \gamma_V^2 B_1 B_2 B_6 B_7 e_2 y_1 y_2 y_3 (1 - \omega), \\ K_7 = \Pi_H \Pi_V \phi^2 \beta_V \beta_H B_6 \rho e_1 e_4 (1 - \omega), \\ K_8 = \Pi_H \Pi_V \phi^2 \beta_V \beta_H B_6 \rho e_1 e_3 (B_1 - \alpha \omega), \\ K_9 = \Pi_H^2 B_7 \gamma_V (\phi \beta_V B_6 e_1 (B_1 - \alpha \omega) + \gamma_V (1 - \omega) e_2) B_1 B_2 B_6 y_1 y_2 y_3, \\ K_{10} = \Pi_H^2 \gamma_V^2 (e_2 (B_1 - \alpha \omega) + B_2 B_6 y_1 y_2 y_3 (1 - \omega)) B_1 B_2 B_6 B_7 y_1 y_2 y_3, \\ K_{11} = \Pi_H \Pi_V \phi^2 \beta_V \beta_H B_6 \rho e_1 (B_1 B_2 B_6 \gamma_H Q_1 (1 - \omega) + e_4 (B_1 - \alpha \omega)), \\ e_1 = \eta y_4 (y_2 y_3 + \sigma y_5 (y_3 + v y_6)), \\ e_2 = B_6 (y_1 y_2 y_3 + \eta y_4 (y_2 y_3 + \sigma y_5 (y_3 + v y_6))) + \eta Q_2, \\ e_3 = (1 - \omega) (B_2 B_6 Q_1 - \kappa \eta Q_2), \\ e_4 = B_2 B_6 Q_1 ((1 - \omega) B_1 + \gamma_H) - \kappa \eta Q_2 (B_1 - \alpha \omega), \\ y_1 = B_3 + (\sigma + \gamma_H) Z_1, y_2 = B_4 + (v + \gamma_H) Z_2, y_3 = B_5 + \gamma_H Z_3,$$

$$y_4 = 1 + Z_1, y_5 = 1 + Z_2, y_6 = 1 + Z_3.$$

For the case when  $\varepsilon = 0$ , the polynomial (11) is reduced to

$$f_{\varepsilon=0}(\lambda_H^{**}) = M_1 \lambda_H^{**4} + M_2 \lambda_H^{**3} + M_3 \lambda_H^{**2} + M_4 \lambda_H^{**} + M_5, \quad (12)$$

where

$$M_1 = \Pi_H^2 B_7 \gamma_V (1 - \omega)^2 (\phi \beta_V B_6 g_1 + \gamma_V g_2) g_2,$$

$$M_2 = H_1 + H_2 - H_3,$$

$$M_3 = H_4 + H_5 + H_6 - (H_7 + H_8),$$

$$M_4 = H_9 + H_{10} - H_{11},$$

$$M_5 = \Pi_H^2 \gamma_V^2 B_1^2 B_2^2 B_3^2 B_4^2 B_5^2 B_6^2 B_7 (1 - R_0^2),$$

with

$$H_1 = \Pi_H^2 B_2 B_3 B_4 B_5 B_6 B_7 \gamma_V (1 - \omega)^2 (\phi \beta_V B_6 g_1 + \gamma_V g_2)$$

$$+ \Pi_H^2 B_7 \gamma_V g_2 (B_1 - \alpha \omega) (1 - \omega) (\phi \beta_V B_6 g_1 + \gamma_V g_2),$$

$$H_2 = \Pi_H^2 B_7 \gamma_V (\phi \beta_V B_6 (B_1 - \alpha \omega) g_1 + \gamma_V (1 - \omega) g_2) (1 - \omega) g_2,$$

$$H_3 = \Pi_H \Pi_V \phi^2 \beta_V \beta_H B_6 \rho g_1 g_3 (1 - \omega),$$

$$H_4 = \Pi_H^2 B_7 \gamma_V (1 - \omega) (\phi \beta_V B_6 g_1 + \gamma_V g_2) B_1 B_2 B_3 B_4 B_5 B_6,$$

$$H_5 = \Pi_H^2 B_7 \gamma_V g_2 (B_1 - \alpha \omega) (\phi \beta_V B_6 g_1 (B_1 - \alpha \omega) + \gamma_V g_2 (1 - \omega))$$

$$+ \Pi_H^2 B_2 B_3 B_4 B_5 B_6 B_7 \gamma_V (1 - \omega) (\phi \beta_V B_6 g_1 (B_1 - \alpha \omega) + \gamma_V g_2 (1 - \omega)),$$

$$H_6 = \Pi_H^2 \gamma_V^2 B_1 B_2 B_3 B_4 B_5 B_6 B_7 g_2 (1 - \omega),$$

$$H_7 = \Pi_H \Pi_V \phi^2 \beta_V \beta_H B_6 \rho g_1 g_4 (1 - \omega),$$

$$H_8 = \Pi_H \Pi_V \phi^2 \beta_V \beta_H B_6 \rho g_1 g_3 (B_1 - \alpha \omega),$$

$$H_9 = \Pi_H^2 B_7 \gamma_V (\phi \beta_V B_6 g_1 (B_1 - \alpha \omega) + \gamma_V (1 - \omega) g_2) B_1 B_2 B_3 B_4 B_5 B_6,$$

$$H_{10} = \Pi_H^2 \gamma_V^2 (g_2 (B_1 - \alpha \omega) + B_2 B_3 B_4 B_5 B_6 (1 - \omega)) B_1 B_2 B_3 B_4 B_5 B_6 B_7,$$

$$H_{11} = \Pi_H \Pi_V \phi^2 \beta_V \beta_H B_6 \rho g_1 (B_1 B_2 B_3 B_4 B_5 B_6 \gamma_H (1 - \omega) + g_4 (B_1 - \alpha \omega)).$$

$$g_1 = \eta (B_4 B_5 + \sigma (B_5 + v)),$$

$$g_2 = B_6 (B_3 B_4 B_5 + \eta (B_4 B_5 + \sigma (B_5 + v))) + \eta (\tau_1 B_4 B_5 + \sigma (\tau_2 B_5 + \tau_3 v)),$$

$$g_3 = (1 - \omega) (B_2 B_3 B_4 B_5 B_6 - \kappa \eta (\tau_1 B_4 B_5 + \sigma (\tau_2 B_5 + \tau_3 v))),$$

$$g_4 = B_2 B_3 B_4 B_5 B_6 ((1 - \omega) B_1 + \gamma_H)$$

$$- \kappa\eta (B_1 - \alpha\omega) (\tau_1 B_4 B_5 + \sigma (\tau_2 B_5 + \tau_3 v)).$$

Clearly, in the polynomial (12)  $M_1 > 0$  (since all the model parameters are positive) and  $M_5 > 0$  whenever  $R_0^2 < 1$  ( $R_0 < 1$ ). Therefore, the number of possible positive real roots of the polynomial (12) can be determined depending on the signs of  $M_2$ ,  $M_3$ , and  $M_4$ . Using the Descartes' rule of signs [31] on the polynomial  $f_{\varepsilon=0}(\lambda_H^{**}) = M_1\lambda_H^{**4} + M_2\lambda_H^{**3} + M_3\lambda_H^{**2} + M_4\lambda_H^{**} + M_5$ , the following result is established.

**Theorem 3.** The LF model (1)

(a) has a unique endemic equilibrium if  $R_0 > 1$  and either of the following conditions holds:

- (i)  $M_2 > 0, M_3 > 0, M_4 > 0,$
- (ii)  $M_2 < 0, M_3 < 0, M_4 < 0,$
- (iii)  $M_2 > 0, M_3 < 0, M_4 < 0,$
- (iv)  $M_2 > 0, M_3 > 0, M_4 < 0;$

(b) Could have more than one endemic equilibrium if  $R_0 > 1$  and either of the following conditions holds:

- (i)  $M_2 < 0, M_3 > 0, M_4 < 0,$
- (ii)  $M_2 < 0, M_3 < 0, M_4 > 0,$
- (iii)  $M_2 > 0, M_3 < 0, M_4 > 0,$
- (iv)  $M_2 < 0, M_3 > 0, M_4 > 0;$

(c) Could have two or more endemic equilibria if  $R_0 < 1$  and any, or all of  $M_2$ ,  $M_3$ , and  $M_4$  are negative.

In case (c) of Theorem 3, multiple endemic equilibria exist when the reproduction number ( $R_0$ ) is less than one (which is a feature of the phenomenon of backward bifurcation). The phenomenon of backward bifurcation is characterized by the co-existence of a stable DFE and a stable endemic equilibrium when the basic reproduction number of the model is less than unity (as observed in numerous epidemiological models, such as [16, 14, 25, 11]). Biologically, the implication of the backward bifurcation is that the necessary

condition for the effective control of LF in the population when the basic reproduction number is less than unity ( $R_0 < 1$ ) is no longer sufficient [26]. The presence of the phenomenon of backward bifurcation in the LF model (1) is investigated in the subsequent section.

### 3.5 Bifurcation analysis

**Theorem 4** (Castillo-Chavez and Song theorem). Let us consider a general system of ordinary differential equations with a parameter  $\varphi$ ,

$$\frac{dx}{dt} = f(x, \varphi), f: \mathbb{R}^n \times \mathbb{R} \rightarrow \mathbb{R}^n, f \in \mathbf{C}^2(\mathbb{R}^n \times \mathbb{R}), \quad (13)$$

where  $x = 0$  is an equilibrium point for the system in (11). That is,  $f(0, \varphi) \equiv 0$  for all  $\varphi$ . Assume the following conditions:

$H_1$ :  $A = D_x f(0, 0) = \left[ \frac{\partial f}{\partial x}(0, 0) \right]$  is the linearization matrix of the system given by (13) around the equilibrium 0 with  $\varphi$  evaluated at 0. Zero is a simple eigenvalue of  $A$  and other eigenvalues of  $A$  have negative real parts.

$H_2$ : Matrix  $A$  has a nonnegative right eigenvector  $w$  and a left eigenvector  $v$  corresponding to the zero eigenvalue.

Let  $f_k$  be the  $k$ th component of  $f$  and let

$$\begin{aligned} a &= \sum_{k,i,j=1}^n v_k w_i w_j \frac{\partial^2 f_k}{\partial x_i \partial x_j}(0, 0), \\ b &= \sum_{k,i=1}^n v_k w_i \frac{\partial^2 f_k}{\partial x_i \partial \varphi}(0, 0). \end{aligned} \quad (14)$$

The local dynamics of (13) around 0 are totally determined by the sign of  $a$  and  $b$ .

1.  $a > 0, b > 0$ ; When  $\varphi < 0$  with  $|\varphi| \ll 1$ , 0 is locally asymptotically stable and there exists a positive unstable equilibrium; when  $0 < \varphi \ll 1$ , 0 is unstable and there exists a negative, locally asymptotically stable equilibrium.

2.  $a < 0, b < 0$ ; When  $\varphi < 0$  with  $|\varphi| \ll 1$ , 0 is unstable; when  $0 < \varphi \ll 1$ , 0 is locally asymptotically stable equilibrium, and there exists a positive unstable equilibrium.
3.  $a > 0, b < 0$ ; When  $\varphi < 0$  with  $|\varphi| \ll 1$ , 0 is unstable, and there exists a locally asymptotically stable negative equilibrium; when  $0 < \varphi \ll 1$ , 0 is stable and a positive unstable equilibrium appears.
4.  $a < 0, b > 0$ ; When  $\varphi$  changes from negative to positive, 0 changes its stability from stable to unstable. Correspondingly, a negative unstable equilibrium becomes positive and locally asymptotically stable.

In particular, if  $a < 0$  and  $b > 0$ , then the bifurcation is forward; if  $a > 0$  and  $b > 0$ , then the bifurcation is backward. Using this approach, the following result may be obtained.

**Theorem 5.** The model of system (1) exhibits backward bifurcation at  $R_0 = 1$ .

*Proof.* We explore the nature of the bifurcation using the center manifold theory [16, 6]. To apply this theory, it is important to carry out the following change of variables. Let  $S_H = x_1, S_{HP} = x_2, E_H = x_3, L = x_4, A = x_5, C = x_6, T = x_7, S_V = x_8, E_V = x_9, I_V = x_{10}$ .

So that

$$N_H = \sum_{i=1}^7 x_i.$$

Furthermore, using the vector notation  $x = (x_1, x_2, x_3, \dots, x_{10})^T$  and  $\frac{dx}{dt} = F(x)$ , with  $F = (f_1, f_2, f_3, \dots, f_{10})^T$ . The LF model (1) can be rewritten as follows:

$$\begin{aligned} \frac{dx_1}{dt} &\equiv f_1 = \Pi_H - \frac{\phi\beta_H x_{10} x_1}{x_1 + x_2 + x_3 + x_4 + x_5 + x_6 + x_7} - (\alpha + \gamma_H) x_1 + \kappa x_7, \\ \frac{dx_2}{dt} &\equiv f_2 = \alpha x_1 - \frac{(1 - \omega) \phi\beta_H x_{10} x_2}{x_1 + x_2 + x_3 + x_4 + x_5 + x_6 + x_7} - \gamma_H x_2, \\ \frac{dx_3}{dt} &\equiv f_3 = \frac{\phi\beta_H x_{10} (x_1 + (1 - \omega) x_2)}{x_1 + x_2 + x_3 + x_4 + x_5 + x_6 + x_7} - (\eta + \gamma_H) x_3, \\ \frac{dx_4}{dt} &\equiv f_4 = \eta x_3 - \frac{\tau_1 x_4}{1 + \varepsilon x_4} - (\sigma + \gamma_H) x_4, \\ \frac{dx_5}{dt} &\equiv f_5 = \sigma x_4 - \frac{\tau_2 x_5}{1 + \varepsilon x_5} - (v + \gamma_H) x_5, \end{aligned}$$

$$\begin{aligned}
\frac{dx_6}{dt} &\equiv f_6 = vx_5 - \frac{\tau_3 x_6}{1 + \varepsilon x_6} - \gamma_H x_6, \\
\frac{dx_7}{dt} &\equiv f_7 = \frac{\tau_1 x_4}{1 + \varepsilon x_4} + \frac{\tau_2 x_5}{1 + \varepsilon x_5} + \frac{\tau_3 x_6}{1 + \varepsilon x_6} - (\kappa + \gamma_H) x_7, \\
\frac{dx_8}{dt} &\equiv f_8 = \Pi_V - \frac{\phi \beta_V (x_4 + x_5 + x_6) x_8}{x_1 + x_2 + x_3 + x_4 + x_5 + x_6 + x_7} - \gamma_V x_8, \\
\frac{dx_9}{dt} &\equiv f_9 = \frac{\phi \beta_V (x_4 + x_5 + x_6) x_8}{x_1 + x_2 + x_3 + x_4 + x_5 + x_6 + x_7} - (\rho + \gamma_V) x_9, \\
\frac{dx_{10}}{dt} &\equiv f_{10} = \rho x_9 - \gamma_V x_{10}.
\end{aligned} \tag{15}$$

Consider the transmission probability  $\beta_H$  as the bifurcation parameter. Solving for  $\beta_H = \beta_H^*$  from  $R_0 = 1$  gives

$$\beta_H = \beta_H^* = \frac{\Pi_H \gamma_V B_1 B_2 B_3 B_4 B_5 B_7}{\Pi_V \gamma_H \phi^2 \beta_V (\gamma_H + (1 - \omega) \alpha) (\sigma (v + B_5) + B_4 B_5) \eta \rho}.$$

Evaluating the Jacobian of the transformed system (15) at DFE  $(\xi_0)$  with  $\beta_H = \beta_H^*$ , is given by

$$J(\xi_0)|_{\beta_H=\beta_H^*} = \begin{bmatrix} -B_1 & 0 & 0 & 0 & 0 & 0 & \kappa & 0 & 0 & -\frac{\phi\beta_H^*\gamma_H}{B_1} \\ \alpha & -\gamma_H & 0 & 0 & 0 & 0 & 0 & 0 & 0 & -\frac{\phi\beta_H^*D_1}{B_1} \\ 0 & 0 & -B_2 & 0 & 0 & 0 & 0 & 0 & 0 & -\frac{\phi\beta_H^*D_2}{B_1} \\ 0 & 0 & \eta & -B_3 & 0 & 0 & 0 & 0 & 0 & 0 \\ 0 & 0 & 0 & \sigma & -B_4 & 0 & 0 & 0 & 0 & 0 \\ 0 & 0 & 0 & 0 & \nu & -B_5 & 0 & 0 & 0 & 0 \\ 0 & 0 & 0 & \tau_1 & \tau_2 & \tau_3 & -B_6 & 0 & 0 & 0 \\ 0 & 0 & 0 & -D_3 & -D_3 & -D_3 & 0 & -\gamma_V & 0 & 0 \\ 0 & 0 & 0 & D_3 & D_3 & D_3 & 0 & 0 & -B_7 & 0 \\ 0 & 0 & 0 & 0 & 0 & 0 & 0 & 0 & \rho & -\gamma_V \end{bmatrix},$$

where

$$B_1 = \alpha + \gamma_H, B_2 = \eta + \gamma_H, B_3 = \sigma + \tau_1 + \gamma_H, B_4 = v + \tau_2 + \gamma_H, B_5 = \tau_3 + \gamma_H, B_6 = \kappa + \gamma_H, B_7 = \rho + \gamma_V, D_1 = (1 - \omega)\alpha, D_2 = \gamma_H + (1 - \omega)\alpha, \text{ and } D_3 = \frac{\phi\beta_H^*\Pi_V\gamma_H}{\Pi_H\gamma_V}.$$

The right eigenvector,  $w = (w_1, w_2, w_3, w_4, w_5, w_6, w_7, w_8, w_9, w_{10})^T$ , associated with the simple zero eigenvalue can be obtained from  $J(\xi_0)|_{\beta_H=\beta_H^*} w = 0$ , given by

$$\begin{aligned} -B_1w_1 + \kappa w_7 - \frac{\phi\beta_H^*\gamma_H}{B_1}w_{10} &= 0, \\ \alpha w_1 - \gamma_H w_2 - \frac{\phi\beta_H^*D_1}{B_1}w_{10} &= 0, \\ -B_2w_3 + \frac{\phi\beta_H^*D_2}{B_1}w_{10} &= 0, \\ \eta w_3 - B_3w_4 &= 0, \\ \sigma w_4 - B_4w_5 &= 0, \end{aligned}$$

$$\begin{aligned}
vw_5 - B_5w_6 &= 0, \\
\tau_1w_4 + \tau_2w_5 + \tau_3w_6 - B_6w_7 &= 0, \\
-\frac{\phi\beta_V\Pi_V\gamma_H}{\Pi_H\gamma_V}w_4 - \frac{\phi\beta_V\Pi_V\gamma_H}{\Pi_H\gamma_V}w_5 - \frac{\phi\beta_V\Pi_V\gamma_H}{\Pi_H\gamma_V}w_6 - \gamma_Vw_8 &= 0, \\
\frac{\phi\beta_V\Pi_V\gamma_H}{\Pi_H\gamma_V}w_4 + \frac{\phi\beta_V\Pi_V\gamma_H}{\Pi_H\gamma_V}w_5 + \frac{\phi\beta_V\Pi_V\gamma_H}{\Pi_H\gamma_V}w_6 - B_7w_9 &= 0, \\
\rho w_9 - \gamma_Vw_{10} &= 0.
\end{aligned} \tag{16}$$

From (16), we obtained

$$\begin{aligned}
w_1 &= \frac{(\kappa\eta D_2 (\tau_1 B_4 B_5 + \tau_2 \sigma B_5 + \tau_3 v \sigma) - \gamma_H B_2 B_3 B_4 B_5)}{B_1 B_3 B_4 B_5 D_2} w_3, \\
w_2 &= \frac{(\alpha \kappa \eta D_2 (\tau_1 B_4 B_5 + \tau_2 \sigma B_5 + \tau_3 v \sigma) - B_2 B_3 B_4 B_5 (\alpha \gamma_H + B_1 D_1))}{\gamma_H B_1 B_3 B_4 B_5 D_2} w_3, \\
w_3 &= w_3 > 0, \quad w_4 = \frac{\eta}{B_3} w_3, \quad w_5 = \frac{\eta \sigma}{B_3 B_4} w_3, \quad w_6 = \frac{\eta v \sigma}{B_3 B_4 B_5} w_3, \\
w_7 &= \frac{\eta (\tau_1 B_4 B_5 + \tau_2 \sigma B_5 + \tau_3 v \sigma)}{B_3 B_4 B_5} w_3, \\
w_8 &= -\frac{\phi \beta_V \Pi_V \gamma_H \eta (B_4 B_5 + \sigma B_5 + v \sigma)}{\Pi_H \gamma_V^2 B_3 B_4 B_5} w_3, \quad w_9 = \frac{\gamma_V B_1 B_2}{\phi \beta_H^* D_2 \rho} w_3, \\
w_{10} &= \frac{B_1 B_2}{\phi \beta_H^* D_2} w_3.
\end{aligned}$$

Similarly, the left eigenvector,  $\nu = (\nu_1, \nu_2, \nu_3, \nu_4, \nu_5, \nu_6, \nu_7, \nu_8, \nu_9, \nu_{10})$ , satisfying  $\nu \cdot w = 1$ , associated with the simple zero eigenvalue can be obtained from  $\nu J(\xi_0)|_{\beta_H = \beta_H^*} = 0$ , given by

$$\begin{aligned}
 & -B_1\nu_1 + \alpha\nu_2 = 0, \\
 & -\gamma_H\nu_2 = 0, \\
 & -B_2\nu_3 + \eta\nu_4 = 0, \\
 & -B_3\nu_4 + \sigma\nu_5 + \tau_1\nu_7 - \frac{\phi\beta_V\Pi_V\gamma_H}{\Pi_H\gamma_V}\nu_8 + \frac{\phi\beta_V\Pi_V\gamma_H}{\Pi_H\gamma_V}\nu_9 = 0, \\
 & -B_4\nu_5 + \nu\nu_6 + \tau_2\nu_7 - \frac{\phi\beta_V\Pi_V\gamma_H}{\Pi_H\gamma_V}\nu_8 + \frac{\phi\beta_V\Pi_V\gamma_H}{\Pi_H\gamma_V}\nu_9 = 0, \\
 & -B_5\nu_6 + \tau_3\nu_7 - \frac{\phi\beta_V\Pi_V\gamma_H}{\Pi_H\gamma_V}\nu_8 + \frac{\phi\beta_V\Pi_V\gamma_H}{\Pi_H\gamma_V}\nu_9 = 0, \\
 & \kappa\nu_1 - B_6\nu_7 = 0, \\
 & -\gamma_V\nu_8 = 0, \\
 & -B_7\nu_9 + \rho\nu_{10} = 0, \\
 & -\frac{\phi\beta_H^*\gamma_H}{B_1}\nu_1 - \frac{\phi\beta_H^*D_1}{B_1}\nu_2 + \frac{\phi\beta_H^*D_2}{B_1}\nu_3 - \gamma_V\nu_{10} = 0.
 \end{aligned} \tag{17}$$

From (17), we obtained

$$\begin{aligned}
 \nu_1 = \nu_2 = \nu_7 = \nu_8 = 0, \quad \nu_3 = \nu_3 > 0, \quad \nu_4 = \frac{B_2}{\eta}\nu_3, \\
 \nu_5 = \frac{\Pi_H\gamma_V B_2 B_3 \nu_3 - \phi\beta_V\Pi_V\gamma_H\eta\nu_9}{\Pi_H\gamma_V\eta\sigma}, \\
 \nu_6 = \frac{\phi\beta_V\Pi_V\gamma_H}{\Pi_H\gamma_V B_5}\nu_9, \nu_9 = \nu_9 > 0, \nu_{10} = \frac{B_7}{\rho}\nu_9.
 \end{aligned}$$

**Computation of  $a$  and  $b$**

Since  $\nu_1 = \nu_2 = \nu_7 = \nu_8 = 0$  for  $k = 1, 2, 3, \dots, 10$ , the only nonzero partial derivatives are

$$\begin{aligned}
 \frac{\partial^2 f_3}{\partial x_1 \partial x_{10}} &= \frac{\partial^2 f_3}{\partial x_{10} \partial x_1} = \frac{\phi\beta_H^*\gamma_H (B_1 - \gamma_H - (1 - \omega)\alpha)}{\Pi_H B_1}, \\
 \frac{\partial^2 f_3}{\partial x_2 \partial x_{10}} &= \frac{\partial^2 f_3}{\partial x_{10} \partial x_2} = \frac{\phi\beta_H^*\gamma_H ((1 - \omega)(B_1 - \alpha) - \gamma_H)}{\Pi_H B_1}, \\
 \frac{\partial^2 f_3}{\partial x_3 \partial x_{10}} &= \frac{\partial^2 f_3}{\partial x_{10} \partial x_3} = \frac{\partial^2 f_3}{\partial x_4 \partial x_{10}} = \frac{\partial^2 f_3}{\partial x_{10} \partial x_4} = \frac{\partial^2 f_3}{\partial x_5 \partial x_{10}} = \frac{\partial^2 f_3}{\partial x_{10} \partial x_5} \\
 &= \frac{\partial^2 f_3}{\partial x_6 \partial x_{10}} = \frac{\partial^2 f_3}{\partial x_{10} \partial x_6} = \frac{\partial^2 f_3}{\partial x_7 \partial x_{10}} = \frac{\partial^2 f_3}{\partial x_{10} \partial x_7} \\
 &= -\frac{\phi\beta_H^*\gamma_H (\gamma_H - (1 - \omega)\alpha)}{\Pi_H B_1}, \\
 \frac{\partial^2 f_9}{\partial x_1 \partial x_4} &= \frac{\partial^2 f_9}{\partial x_4 \partial x_1} = \frac{\partial^2 f_9}{\partial x_2 \partial x_4} = \frac{\partial^2 f_9}{\partial x_4 \partial x_2} = \frac{\partial^2 f_9}{\partial x_3 \partial x_4} = \frac{\partial^2 f_9}{\partial x_4 \partial x_3} = \frac{\partial^2 f_9}{\partial x_4 \partial x_7}
 \end{aligned} \tag{18}$$

$$\begin{aligned}
 &= \frac{\partial^2 f_9}{\partial x_7 \partial x_4} = -\frac{\phi \beta_V \Pi_V \gamma_H^2}{\Pi_H^2 \gamma_V}, \\
 \frac{\partial^2 f_9}{\partial x_4^2} &= \frac{\partial^2 f_9}{\partial x_4 \partial x_5} = \frac{\partial^2 f_9}{\partial x_5 \partial x_4} = \frac{\partial^2 f_9}{\partial x_4 \partial x_6} = \frac{\partial^2 f_9}{\partial x_6 \partial x_4} = -\frac{2\phi \beta_V \Pi_V \gamma_H^2}{\Pi_H^2 \gamma_V}, \\
 \frac{\partial^2 f_9}{\partial x_1 \partial x_5} &= \frac{\partial^2 f_9}{\partial x_5 \partial x_1} = \frac{\partial^2 f_9}{\partial x_2 \partial x_5} = \frac{\partial^2 f_9}{\partial x_5 \partial x_2} = \frac{\partial^2 f_9}{\partial x_3 \partial x_5} = \frac{\partial^2 f_9}{\partial x_5 \partial x_3} = \frac{\partial^2 f_9}{\partial x_5 \partial x_7} \\
 &= \frac{\partial^2 f_9}{\partial x_7 \partial x_5} = -\frac{\phi \beta_V \Pi_V \gamma_H^2}{\Pi_H^2 \gamma_V}, \quad \frac{\partial^2 f_9}{\partial x_5^2} = \frac{\partial^2 f_9}{\partial x_6^2} = \frac{\partial^2 f_9}{\partial x_5 \partial x_6} \\
 &= \frac{\partial^2 f_9}{\partial x_6 \partial x_5} = -\frac{2\phi \beta_V \Pi_V \gamma_H^2}{\Pi_H^2 \gamma_V}, \\
 \frac{\partial^2 f_9}{\partial x_1 \partial x_6} &= \frac{\partial^2 f_9}{\partial x_6 \partial x_1} = \frac{\partial^2 f_9}{\partial x_2 \partial x_6} = \frac{\partial^2 f_9}{\partial x_6 \partial x_2} = \frac{\partial^2 f_9}{\partial x_3 \partial x_6} = \frac{\partial^2 f_9}{\partial x_6 \partial x_3} = \frac{\partial^2 f_9}{\partial x_6 \partial x_7} \\
 &= \frac{\partial^2 f_9}{\partial x_7 \partial x_6} = -\frac{\phi \beta_V \Pi_V \gamma_H^2}{\Pi_H^2 \gamma_V}, \\
 \frac{\partial^2 f_9}{\partial x_4 \partial x_8} &= \frac{\partial^2 f_9}{\partial x_8 \partial x_4} = \frac{\partial^2 f_9}{\partial x_5 \partial x_8} = \frac{\partial^2 f_9}{\partial x_8 \partial x_5} = \frac{\partial^2 f_9}{\partial x_6 \partial x_8} = \frac{\partial^2 f_9}{\partial x_8 \partial x_6} = \frac{\partial^2 f_9}{\partial x_6 \partial x_7} \\
 &= \frac{\partial^2 f_9}{\partial x_7 \partial x_6} = \frac{\phi \beta_V \gamma_H}{\Pi_H}, \quad \frac{\partial^2 f_3}{\partial x_{10} \partial \beta_H^*} = \frac{\phi (\gamma_H + (1 - \omega) \alpha)}{B_1}, \quad (19)
 \end{aligned}$$

but

$$\begin{aligned}
 a &= \sum_{k,i,j=1}^n v_k w_i w_j \frac{\partial^2 f_k}{\partial x_i \partial x_j} (0, 0), \\
 a &= -\frac{2\nu_3 w_3^2 \gamma_H (\gamma_H - (1 - \omega) \alpha) B_2 \Theta_1}{\Pi_H B_3 B_4 B_5 D_2} \\
 &+ \frac{2\nu_3 w_3^2 \gamma_H (B_1 - \gamma_H - (1 - \omega) \alpha) B_2 \Theta_2}{\Pi_H B_1 B_3 B_4 B_5 D_2^2} \\
 &+ \frac{2\nu_3 w_3^2 ((1 - \omega) (B_1 - \alpha) - \gamma_H) B_2 \Theta_3}{\Pi_H B_1 B_3 B_4 B_5 D_2^2} \\
 &- \frac{2\nu_9 w_3^2 \phi \beta_V \Pi_V \gamma_H^2 \eta (B_4 B_5 + \sigma B_5 + v\sigma) \Theta_1}{\Pi_H^2 \gamma_V B_3^2 B_4^2 B_5^2} \\
 &- \frac{2\nu_9 w_3^2 \phi \beta_V \Pi_V \gamma_H^2 \eta (B_4 B_5 + \sigma B_5 + v\sigma) \Theta_2}{\Pi_H^2 \gamma_V B_1 B_3^2 B_4^2 B_5^2 D_2} \\
 &- \frac{2\nu_9 w_3^2 \phi \beta_V \Pi_V \gamma_H \eta (B_4 B_5 + \sigma B_5 + v\sigma) \Theta_3}{\Pi_H^2 \gamma_V B_1 B_3^2 B_4^2 B_5^2 D_2} \\
 &- \frac{2\nu_9 w_3^2 \phi \beta_V \Pi_V \gamma_H^2 \eta^2 (B_4 B_5 + \sigma B_5 + v\sigma)^2}{\Pi_H^2 \gamma_V^2 B_3^2 B_4^2 B_5^2}, \quad (20)
 \end{aligned}$$

where

$$\begin{aligned} \Theta_1 &= B_3B_4B_5 + \eta(B_4B_5(1 + \tau_1) + \sigma B_5(1 + \tau_2) + v\sigma(1 + \tau_3)), \\ \Theta_2 &= \kappa\eta D_2(\tau_1B_4B_5 + \tau_2\sigma B_5 + \tau_3v\sigma) - \gamma_H B_2B_3B_4B_5, \\ \Theta_3 &= \alpha\kappa\eta D_2(\tau_1B_4B_5 + \tau_2\sigma B_5 + \tau_3v\sigma) - B_2B_3B_4B_5(\alpha\gamma_H + B_1D_1). \end{aligned}$$

Similarly, we calculate for  $b$ , given by

$$\begin{aligned} b &= \sum_{k,i=1}^n v_k w_i \frac{\partial^2 f_k}{\partial x_i \partial \beta^*}(0, 0), \\ b &= \frac{\nu_3 w_3 B_2}{\beta_H^*} > 0, \end{aligned} \tag{21}$$

Hence, since the bifurcation coefficient  $b$  is positive and the sign of the coefficient of  $a$  is positive, it follows, from Theorem 5 that the LF model exhibits a backward bifurcation at  $R_0 = 1$ . Figure 2 shows the backward bifurcation diagram of the LF model (1).  $\square$

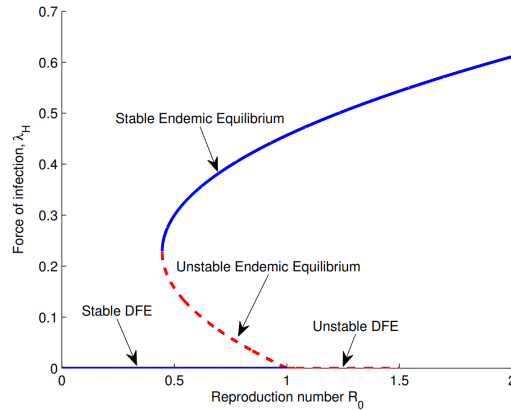


Figure 2: Backward bifurcation diagram of the LF model (1), showing the profile of the force of infection ( $\lambda_H^{**}$ ) as a function of the reproduction number ( $R_0$ ). The parameter values used are as in Table 2, (so that  $a = 1.4006 \times 10^{-4}$ ).

## 4 Numerical simulations

In this section, we carry out the numerical simulations of the LF model (1) using parameter values in Table 2, so as to illustrate some of the analytic results obtained in this study.

Table 2: Parameters value of the LF model (1)

Paramter	Value	Source
$\Pi_H$	0.01747	[4]
$\Pi_V$	100	[16]
$\phi$	0.45	[4]
$\beta_H$	0.01	[28]
$\beta_V$	0.1	[28]
$\gamma_H$	0.000039	[21]
$\gamma_V$	0.1439	[21]
$\alpha$	0.1	Assumed
$\sigma$	0.45	Assumed
$\omega$	0.2	Assumed
$\eta$	0.00238	[21]
$\nu$	0.48	Assumed
$\tau_1$	0.2	Assumed
$\tau_2$	0.3	Assumed
$\tau_3$	0.5	Assumed
$\varepsilon$	0.5	Assumed
$\kappa$	0.135	Assumed
$\rho$	0.0555	[21]

### 4.1 Discussion

In Figure 3, each surface represents the value of the basic reproduction number as a function of two parameters. In Figure 3e, it is shown that the basic reproduction number increases very fast as the mosquito-biting rate

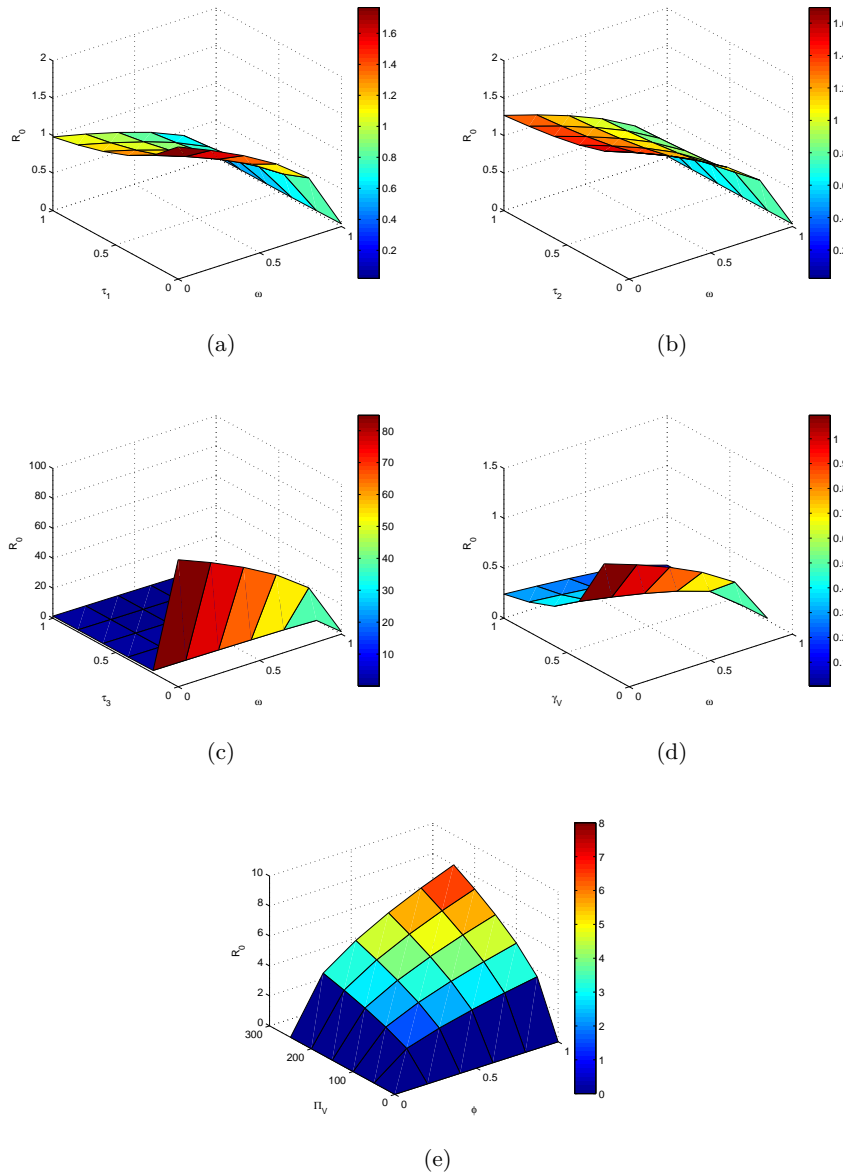
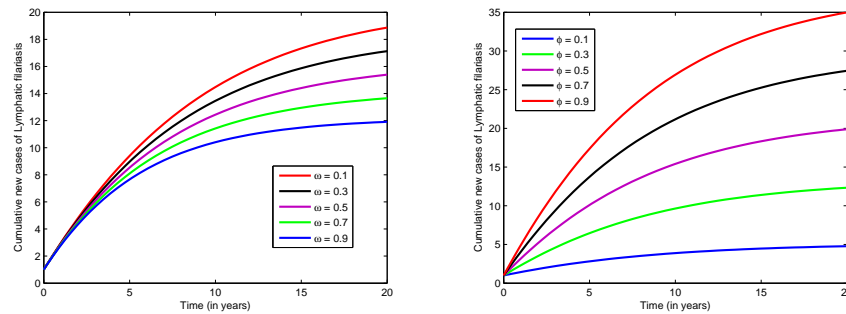


Figure 3: Surface plots of the basic reproduction number with respect to (a)  $\omega$  and  $\tau_1$  (b)  $\omega$  and  $\tau_2$  (c)  $\omega$  and  $\tau_3$  (d)  $\omega$  and  $\gamma_V$  (e)  $\phi$  and  $\Pi_V$ .

and vector recruitment rate increase. In Figure 3c, the surface of the basic reproduction number diminishes as the value of the treatment rate for

Chronic stage infected individuals and the efficacy of the prophylaxis drugs increases. It is observed in Figure 3a and 3b that the surface of the basic reproduction number increases as the treatment rates and the efficacy of prophylaxis drugs decrease. In Figure 3d, the surface of the basic reproduction number decreases as the vector death rate and efficacy of prophylaxis drugs increases.

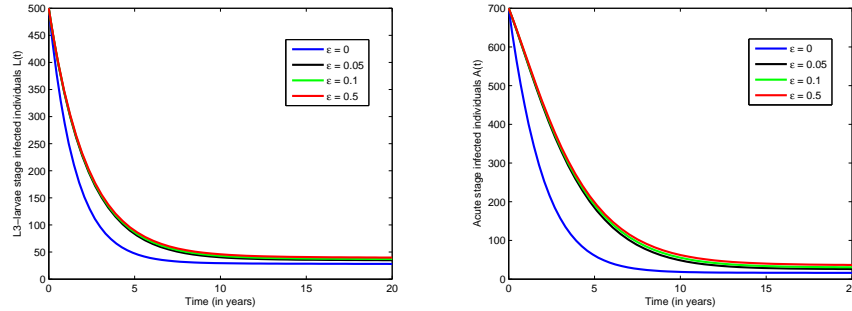


(a) The effect of  $\omega$  on the Cumulative new cases of LF. (b) The effect of  $\phi$  on the Cumulative new cases of LF.

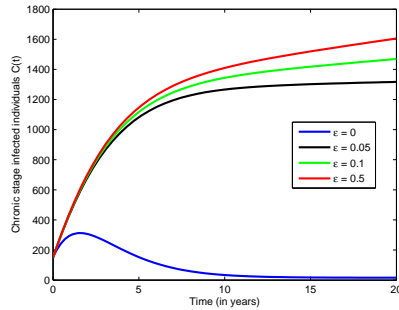
Figure 4: Effect of  $\omega$  and  $\phi$  on the Cumulative new cases of LF

Figure 4a depicts the simulation of the effect of efficacy of prophylaxis drugs ( $\omega$ ) on the cumulative new cases of LF. It is observed that as the rate of the efficacy of prophylaxis drugs ( $\omega$ ) increases, there is a decrease in the number of the cumulative new cases of LF. Figure 4b is the simulation of the effect of the mosquito-biting rate ( $\phi$ ) on the cumulative new cases of LF, it is shown that as the mosquito-biting rate ( $\phi$ ) increases, the number of the cumulative new cases of LF increases as well.

Figure 5 depicts the simulations of the effect of the limitation rate in medical resources availability ( $\varepsilon$ ) on the infected classes respectively while the treatment rates are constant. It is observed that the limitation rate in medical resources availability has a significant impact on the increase and decrease of infected individuals, especially in the chronic stage of infection. In Figure 5a, when  $\varepsilon = 0$ , the number of L3-larvae stage infected individuals was low compared to when  $\varepsilon = 0.05$ ,  $\varepsilon = 0.1$ , and  $\varepsilon = 0.5$ , we observed a similar result in Figure 5b. In Figure 5c, when  $\varepsilon = 0$ , the chronic stage



(a) The effect of  $\epsilon$  on L3-larvae stage infected individuals. (b) The effect of  $\epsilon$  on Acute stage infected individuals.



(c) The effect of  $\epsilon$  on Chronic stage infected individuals.

Figure 5: Effect of  $\epsilon$  on the infected compartments.

infected individuals reduce from 200 to almost less than 10 in eight years, but when  $\epsilon = 0.05$ ,  $\epsilon = 0.1$ , and  $\epsilon = 0.5$ , it was observed that the chronic stage infected individuals increase tremendously.

In Figure 6, we simulate the effect of the treatment rate ( $\tau_1$ ) on the L3-larvae stage infected individuals with various values for the limitation rate in medical resources availability ( $\epsilon$ ). In Figure 6a, it is observed that when  $\epsilon = 0$ , and the treatment rate is varied ( $\tau_1$ ) to 0.9 the number of L3-larvae stage infected individuals reduced from 500 to less than 50 in 2 years. Whereas, in Figure 6b, when  $\epsilon = 0.01$ , it took about 3.2 years for the

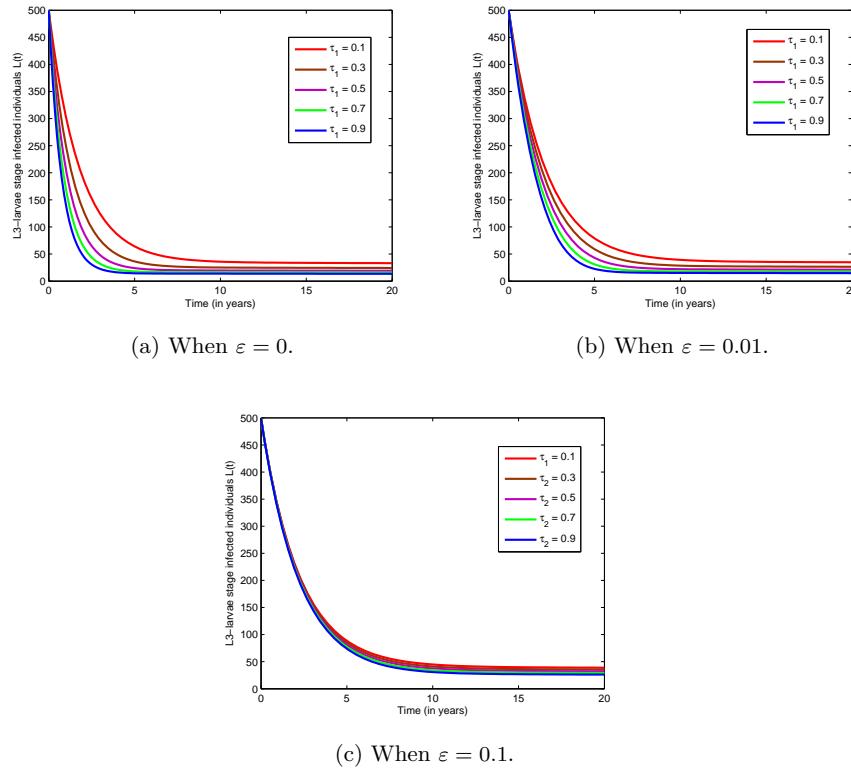


Figure 6: The effect of the treatment rate ( $\tau_1$ ) on the L3-larvae stage infected individuals.

infected individuals to be less than 50. In Figure 6c it took about 6 years for the number of infected individuals to be less than 50, when  $\varepsilon = 0.1$ .

Similarly, Figure 7 depicts simulations of the effect of treatment rate ( $\tau_2$ ) on the Acute stage infected individuals with various values for the limitation rate in medical resources availability ( $\varepsilon$ ). It is observed in Figure 7a that when  $\varepsilon = 0$ , and the treatment rate ( $\tau_2$ ) is varied to 0.9 the number of Acute stage infected individuals reduced from 700 to less than 100 in 2 years. Whereas, in Figure 7b, when  $\varepsilon = 0.01$ , it took about 4 years for the infected individuals to be less than 100. In Figure 7c it took about 6.5 years for the number of infected individuals to be less than 100, when  $\varepsilon = 0.1$ . Figure 8 depicts simulations of the effect of treatment rate ( $\tau_3$ ) on the Chronic stage infected individuals with various values for the limitation rate in medical resources

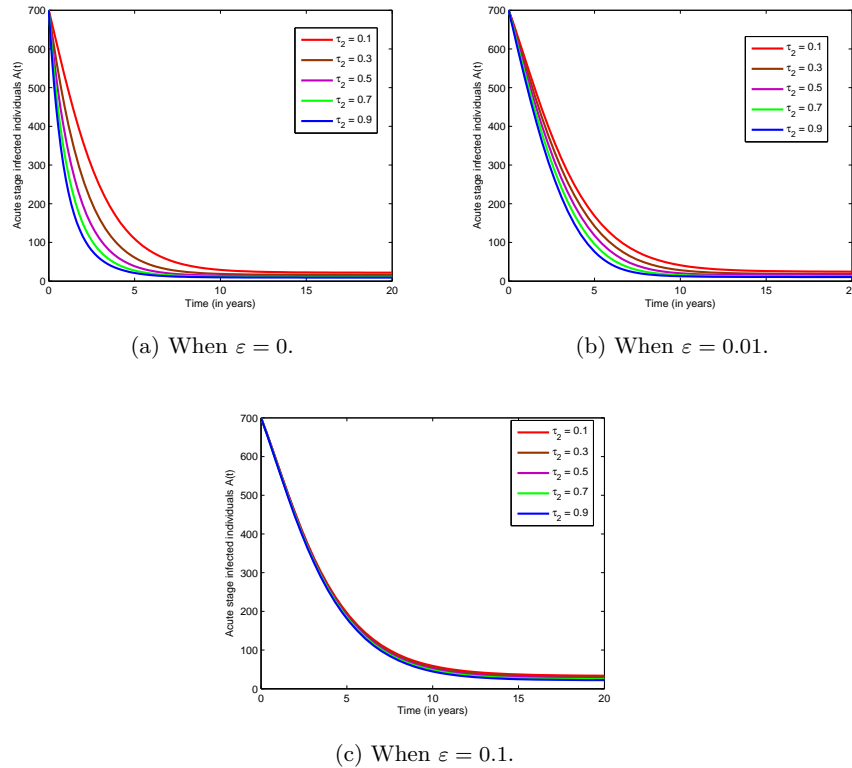


Figure 7: The effect of the treatment rate ( $\tau_2$ ) on the Acute stage infected individuals.

availability ( $\varepsilon$ ). In Figure 8a, it is observed that when the treatment rate ( $\tau_3$ ) is varied to 0.9 and  $\varepsilon = 0$ , the number of chronic stage infected individual reduces from 200 to zero within 10 years, but in Figure 8b it took up to 20 years to reduce the number of infected to be less than 10. It is also observed that in Figure 8a when  $\tau_3 = 0.1$  and  $\varepsilon = 0$ , the number of infected individuals is lower as compared to Figure 8b where  $\tau_3 = 0.1$  and  $\varepsilon = 0.01$ . In Figure 8c, it is observed that when  $\varepsilon = 0.1$ , the treatment rate has minimal effect in reducing the number of infected individuals, and even if the treatment rate is increased to 0.9 the disease will persist and the number of chronic stage infected individuals will keep on increasing.

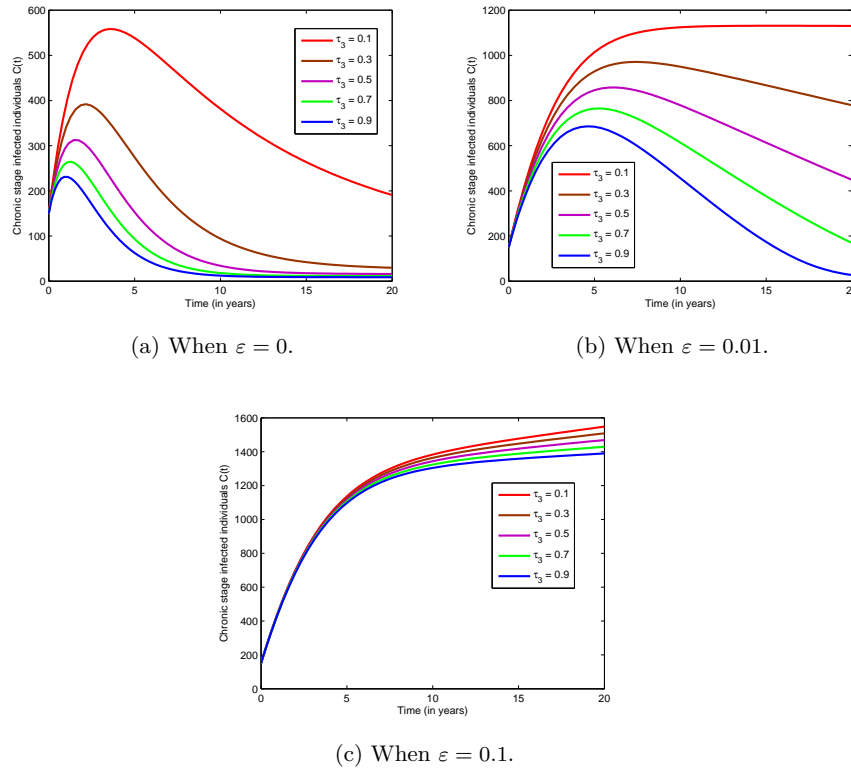


Figure 8: The effect of the treatment rate ( $\tau_3$ ) on the Chronic stage infected individuals.

## 5 Conclusions

In this paper, a deterministic mathematical model with Holling type II treatment functions is presented and rigorously analyzed in order to understand the dynamics of LF. Qualitative analysis of the model shows that the model has a locally asymptotically stable DFE when the basic reproduction number ( $R_0$ ) is less than unity. The study also uncovers that the LF model exhibits the phenomenon of backward bifurcation, characterized by the coexistence of a stable DFE and a stable endemic equilibrium when the basic reproduction number of the model is less than one. From a biological standpoint, the implication of backward bifurcation is that the necessary condition for effectively controlling LF in the population is no longer sufficient when the basic re-

production number is less than one. The numerical simulations demonstrate that increasing treatment rates, availability of medical resources, and efficacy of prophylaxis drugs significantly reduce the burden of LF. It is recommended that policy makers in the healthcare sector should increase the rate of MDA and availability of medical resources as well as mosquito bed nets in rural areas and regions at risk of LF. Sensitization should also be carried out on the importance of testing and sanitation. In future research, there is potential to reformulate the model and include the diurnal periodicity of microfilariae, thus incorporating the periodic nature of disease transmission pathways. Additionally, extending the model to introduce time-dependent optimal control strategies could be explored, allowing for a more nuanced understanding of disease management. Furthermore, investigating the co-dynamics of LF with other infectious diseases would provide valuable insights into the interplay between multiple diseases and their control measures.

## Abbreviations

LF Lymphatic filariasis

DFE Disease-Free Equilibrium

$R_0$  Basic Reproduction Number

## Ethics approval and consent to participate

No ethical approval was required for this manuscript.

## Consent for publication

Not applicable

## Availability of data and material

Not applicable

## Competing interests

The authors declare that they have no competing interests, financial or non-financial, that could be perceived as influencing the content or conclusions of this paper.

## Funding

No funding received for this work

## Authors' contributions

All the authors contributed equally, and approved the final draft of the manuscript

## Acknowledgements

Not applicable

## References

- [1] Al-Tameemi, K. and Kabakli, R.A.I.A.N. *Lymphatic filariasis: an overview*, Asian J. Pharm. Clin. Res., 12 (2019), 1–5.
- [2] Bakowski, M.A. and McNamara, C.W. *Advances in antiwobachial drug discovery for treatment of parasitic filarial worm infections*, Trop. Med. Infect. Dis., 4 (2019), 108.
- [3] Bhunu, C.P. and Mushayabasa, S. *Transmission dynamics of lymphatic filariasis: a mathematical approach*, Int. Scholarly Res. Notices, 2012 (2012), 930130.

- [4] Biswas, S.K., Ghosh, U. and Sarkar, S. *Mathematical model of Zika virus dynamics with vector control and sensitivity analysis*, Infect. Dis. Model., 5 (2020), 23–41.
- [5] Cano, J., Rebollo, M.P., Golding, N., Pullan, R.L., Crellen, T., Soler, A., Hope, L.A.K., Lindsay, S.W., Hay, S.I., Bockarie, M.J. and Brooker, S.J. *The global distribution and transmission limits of lymphatic filariasis: past and present*, Parasites Vectors, 7 (2014), 1–19.
- [6] Castillo-Chavez, C. and Song, B. *Dynamical models of tuberculosis and their applications*, Math. Biosci. Eng., 1 (2004), 361–404.
- [7] Chandy, A., Thakur, A.S., Singh, M.P. and Manigauha, A. *A review of neglected tropical diseases: filariasis*, Asian Pac. J. Trop. Med., 4 (2011), 581–586.
- [8] Das, P.K., Pani, S.P. and Krishnamoorthy, K. *Prospects of elimination of lymphatic filariasis in India*, ICMR Bull., 32 (2002), 41–54.
- [9] Diekmann, O. and Heesterbeek, J.A.P. *Mathematical epidemiology of infectious diseases: model building, analysis and interpretation*, Vol. 5, John Wiley & Sons, 2000.
- [10] Fimbo, A.M., Minzi, O.M., Mmbando, B.P., Barry, A., Nkayamba, A.F., Mwamwitwa, K.W., Malishee, A., Seth, M.D., Makunde, W.H., Gurusurthy, P. and Lusingu, J.P. *Prevalence and correlates of lymphatic filariasis infection and its morbidity following mass ivermectin and albendazole administration in Mkinga District, North-Eastern Tanzania*, J. Clin. Med., 9 (2020), 1550.
- [11] Garba, S.M., Gumel, A.B. and Bakar, M.A. *Backward bifurcations in dengue transmission dynamics*, Math. Biosci., 215 (2008), 11–25.
- [12] Gordon, C.A., Jones, M.K. and McManus, D.P. *The history of Bancroftian lymphatic filariasis in Australasia and Oceania: is there a threat of re-occurrence in mainland Australia?*, Trop. Med. Infect. Dis., 3 (2018), 58.

- [13] Gravis, M. *National Organization for Rare Disorders (NORD)*, Available here, accessed March 2022.
- [14] Gumel, A.B. *Causes of backward bifurcations in some epidemiological models*, J. Math. Anal. Appl., 395 (2012), 355–365.
- [15] Hoerauf, A., Pfarr, K., Mand, S., Debrah, A. Y. and Specht, S. *Filariasis in Africa—treatment challenges and prospects*, Clin. Microbiol. Infect., 17 (2011), 977–985.
- [16] Jose, S.A., Raja, R., Omede, B.I., Agarwal, R.P., Alzabut, J., Cao, J. and Balas, V.E. *Mathematical modeling on co-infection: transmission dynamics of Zika virus and Dengue fever*, Nonlinear Dyn., 111 (2023), 4879–4914.
- [17] Kumar, A. and Nilam *Mathematical analysis of a delayed epidemic model with nonlinear incidence and treatment rates*, J. Eng. Math., 115 (2019), 1–20.
- [18] Lakshmikantham, V., Leela, S. and Martynuk, A.A. *Stability analysis of nonlinear systems*, M. Dekker, New York, (1989) 249–275.
- [19] Medeiros, Z.M., Vieira, A.V., Xavier, A.T., Bezerra, G.S., Lopes, M.D.F.C., Bonfim, C.V. and Aguiar-Santos, A.M. *Lymphatic filariasis: a systematic review on morbidity and its repercussions in countries in the Americas*, Int. J. Environ. Res. Public Health, 19 (2021), 316.
- [20] Melrose, W.D. *Lymphatic filariasis: new insights into an old disease*, Int. J. Parasitol., 32 (2002), 947–960.
- [21] Mwamtobe, P.M., Simelane, S.M., Abelman, S. and Tchuenche, J.M. *Mathematical analysis of a lymphatic filariasis model with quarantine and treatment*, BMC Public Health, 17 (2017), 1–13.
- [22] Negasa, A. and Dufera, M. *Assessment of etiology of elephantiasis and its associated risk factors in Jeldu district, West Shoa, Ethiopia*, J. Trop. Med., (2021) 5551637.

- [23] Oguntolu, F.A., Peter, O.J., Yusuf, A., Omede, B.I., Bolarin, G. and Ayoola, T.A. *Mathematical model and analysis of the soil-transmitted helminth infections with optimal control*, *Model. Earth Syst. Environ.*, 10 (2024), 883–897.
- [24] Oguntolu, F.A., Yavalah, D.W., Udom, C.F., Ayoola, T.A. and Victor, A.A. *A mathematical modelling of lymphatic filariasis and malaria co-infection*, 2022.
- [25] Omede, B.I., Jose, S.A., Anuwat, J. and Park, T. *Mathematical analysis on the transmission dynamics of delta and omicron variants of COVID-19 in the United States*, *Model. Earth Syst. Environ.*, (2024) 1–38.
- [26] Omede, B.I., Odionyenma, U.B., Ibrahim, A.A. and Bolaji, B. *Third wave of COVID-19: mathematical model with optimal control strategy for reducing the disease burden in Nigeria*, *Int. J. Dyn. Control*, 11 (2023), 411–427.
- [27] Stocks, M.E., Freeman, M.C. and Addiss, D.G. *The effect of hygiene-based lymphedema management in lymphatic filariasis-endemic areas: a systematic review and meta-analysis*, *PLoS Negl. Trop. Dis.*, 9 (2015), e0004171.
- [28] Supriatna, A.K. and Anggriani, N. *Lymphatic filariasis transmission and control: a mathematical modelling approach*, in *Current Topics in Tropical Medicine*, (2012) 425–442.
- [29] Van den Driessche, P. and Watmough, J. *Reproduction numbers and sub-threshold endemic equilibria for compartmental models of disease transmission*, *Math. Biosci.*, 180 (2002), 29–48.
- [30] Wang, W. and Ruan, S. *Bifurcations in an epidemic model with constant removal rate of the infectives*, *J. Math. Anal. Appl.*, 291 (2004), 775–793.
- [31] Wang, X. *A simple proof of Descartes’s rule of signs*, *Am. Math. Mon.*, 111 (2004), 525–526.
- [32] World Health Organization. *Preventive chemotherapy in human helminthiasis*, Geneva: World Health Organization, 2006 [online].

- [33] World Health Organization. *Monitoring and epidemiological assessment of mass drug administration in the global programme to eliminate lymphatic filariasis: a manual for national elimination programmes*, World Health Organization, 2011.
- [34] World Health Organization. *Global programme to eliminate lymphatic filariasis: progress report, 2011*, Wkly. Epidemiol. Rec., 87 (2012), 346–356.
- [35] World Health Organization. *Lymphatic filariasis: a handbook of practical entomology for national lymphatic filariasis elimination programmes (No. WHO/HTM/NTD/PCT/2013.10)*, World Health Organization, 2013.
- [36] World Health Organization. *Ending the neglect to attain the Sustainable Development Goals: a road map for neglected tropical diseases 2021–2030*, World Health Organization, 2020.
- [37] Zhou, L. and Fan, M. *Dynamics of an SIR epidemic model with limited medical resources revisited*, Nonlinear Anal. Real World Appl., 13 (2012), 312–324.